WARSAW UNIVERSITY OF TECHNOLOGY Index 351733
FACULTY OF CIVIL ENGINEERING
COMMITTEE FOR CIVIL AND WATER ENGINEERING
POLISH ACADEMY OF SCIENCES ISSN 1230-2945

DOI: 10.24425/ace.2023.145275

ARCHIVES OF CIVIL ENGINEERING

Vol. LXIX ISSUE 2 2023

pp. 399 –416

Research paper

Research on the linear viscoelastic rheological properties of rejuvenated asphalt mastic based on the discrete element method

Mei Lin[1], Yu Lei[2], Ping Li[3], Jun Shuai[4], Zhaoli Wang[5]

Abstract: The rheological property of asphalt is an important factor affecting the pavement performance of asphalt binder, and the fundamental reason for the change of asphalt rheological property is the strong evolution of asphalt material meso structure. However, the internal mechanism of rejuvenated asphalt mastic system is complex and its rules are difficult to grasp. Aiming to study the relationship between meso mechanical parameters and rheological parameters of rejuvenated asphalt mastic, the meso structure model of rejuvenated asphalt mastic was established and improved based on the discrete element method. Moreover, the meso parameters of the model were obtained by the objective function method, and then the influences of various factors were studied to construct the mathematical constitutive model of rheological parameter modulus and meso mechanical parameters. Combing with the reliability of the improved Burgers model was verified based on the rheological test results of rejuvenated asphalt mastic. In addition, the virtual test of dynamic shear rheological dynamic frequency scanning was carried out on the asphalt mastic sample by particle flow software. By adjusting the mesomechanical parameters, the simulation results (complex shear modulus and phase angle) were consistent with the test results. This study clarified the relationship between mesomechanics and macro performance, and this model could be used to obtain the complex shear modulus of rejuvenated asphalt mastic under different types, filler-asphalt ratio and external force environments by adjusting particle flow, wall boundary and other conditions, which can greatly save the workload for the later research and provide a theoretical basis for production experiments.

Keywords: constitutive model, discrete element method, rejuvenated asphalt mastic, rheological characteristics

[1]PhD., School of Civil Engineering, Lanzhou University of Technology, Lanzhou, 730050, China, e-mail: 280759800@qq.com, ORCID: 0000-0002-5348-3769

[2]MA.Eng., School of Civil Engineering, Lanzhou University of Technology, Lanzhou, 730050, China, e-mail: 794868984@qq.com, ORCID: 0000-0001-9836-351X

[3]Prof., PhD., School of Civil Engineering, Lanzhou University of Technology, Lanzhou, 730050, China, e-mail: lzlgliping@126.com, ORCID: 0000-0001-5963-3679

[4]MA.Eng., School of Civil Engineering, Lanzhou University of Technology, Lanzhou, 730050, China, e-mail: 1420553745@qq.com, ORCID: 0000-0002-4187-7250

[5]Eng., Gansu Road and Bridge Green Smart Construction Technology Industry Research Institute, Lanzhou, 730030, China, e-mail: 907165650@qq.com, ORCID: 0000-0002-4073-5250

1. Introduction

Asphalt pavement has many advantages, such as easy to construct, good wear resistance, and high flatness, and its proportion in road engineering has been increasing [1–3]. However, due to the influence of natural environmental factors and vehicle loads, asphalt pavement inevitably suffers from rutting, low-temperature cracking, loosening and other damages, which seriously affects the driving safety and comfort. Therefore, after large-scale construction was completed, asphalt pavement changed from the past road construction era to the maintenance era. However, asphalt pavement maintenance and repair have produced a large amount of Reclaimed Asphalt Pavement (RAP) that need to be treated urgently [4–6]. In the meantime, the raw material resources such as asphalt and aggregate are scarce. Recycling asphalt pavement is the fundamental means to solve the problem, which not only brings economic advantages, but also brings environmental benefits. However, recycling asphalt pavement have great variability of road performance, it is difficult to guarantee the performance of rejuvenated asphalt and rejuvenated asphalt mastic in the recycling process [7]. As a typical viscoelastic fluid material, the physical morphology and mechanical properties of asphalt are greatly affected by temperature. Under the action of low temperature and transient load, the elastic deformation of asphalt takes the main place, while under high temperature and long-term load, the deformation of asphalt is completely close to viscosity. However, in most practical situations, the deformation of asphalt is mainly viscoelastic. All these phenomena are called rheological properties of asphalt, which is also the viscoelastic plastic and flow deformation constitutive properties of asphalt. It can be seen that the rheological property of asphalt is an important factor affecting the performance of asphalt binder. At the same time, the Strategic Highway Research Program (SHRP) plan of the United States proposed that the rheological properties of the asphalt binders are closely related to the actual road performance [8–11]. A lot of research and practice show that asphalt pavement with poor rheology is prone to rutting, cracking and other diseases [12–14]. The fundamental reason for the change of asphalt rheological properties is the great difference of asphalt material mesostructure, which affects the road performance of the asphalt mixture [15, 16]. Therefore, the road performance of the rejuvenated asphalt mixture largely depends on the rheological performance and meso structure of rejuvenated asphalt mastic. Thus, studying the relationship between the rheological performance and meso structure of asphalt is helpful to understand the essential factors influencing the change of asphalt mixture road performance and promote the asphalt recycling [17–20].

In recent years, the mesomechanics method has attracted widespread attention in the field of predicting the performance of asphalt mastic and asphalt mixture. As an important branch of mesomechanics method, discrete element methods (DEM) used by many scholars to establish mesomechanics model of asphalt mixture and analyze mesomechanics [21, 22]. As an important parts of the asphalt mixture, the composition structure and rheological properties of asphalt mastic plays a dominant role in the road performance of the asphalt mixture [4, 5, 23, 26]. Abbas et al [27] established a two-dimensional model based on image recognition technology and DEM, and predicted the Standard Penetration Test Phase Angle of the mixture based on the rheological properties of a variety of bitumen. Liu et al. [28]

studied and obtained the diameter reduction coefficient to control this effect. Ma [29] established a modified Burgers model based on DEM, conducted a virtual dynamic shear rheological (DSR) test, and analyzed the viscoelastic-plastic action in asphalt mastic. Ma et al. [30] used DEM to model the structure of asphalt mastic and revealed the macroscopic response caused by the shape and size of mineral powder particles in asphalt mastic.

There are many studies on meso simulations of asphalt mixtures using the DEM in existing studies, but few studies on asphalt and asphalt mastic, especially on rejuvenated asphalt mastic. In order to study the relationship between the mesoomechanical parameters and rheological parameters of rejuvenated asphalt mastic, this paper used the three-dimensional discrete element particle flow software developed by Itasca to simulate the DSR experiment of asphalt mastic. The improved Burgers model was used to simulate the viscoelastic effect of asphalt mastic. Then, according to the indoor DSR test results, the complex shear modulus and phase angle master curve of different kinds of asphalt mastic DSR tests were fitted. At the same time, the fitting results of Burgers model parameters were analyzed. Finally, the internal mechanism of asphalt and asphalt mastic was revealed from the microscopic perspective through virtual test.

2. Raw materials and performance testing

2.1. Base asphalt

In this study, KL-90 asphalt was selected as the base asphalt, and its basic properties were tested in accordance with the "Highway Engineering Asphalt and Asphalt Mixture Test Regulations" (JTG E20-2011). The results are shown in Table 1.

Table 1. Technical indexes of base asphalt(KL-90)

Name of the pilot project		Unit	Test Results	Requirements
Penetration (25°C, 100 g, 5 s)		mm	85	80÷100
Softening Point		°C	48	≥ 44
Ductility (15°C)		cm	179	≥ 100
RTFOT ageing	Quality change	%	–0.12	–0.8÷0.8
	Residual penetration	%	72	≥ 57
	Residual Dilution (10°C)	cm	21	≥ 8

2.2. Mineral filler

In this paper, the limestone aggregate commonly used in Northwest China was selected, and the aggregate is ground into powder by electromagnetic pulverizer, and then the mineral filler with particle sizes less than 0.075 mm through a 0.075 mm square hole sieve as the sample. In accordance with the "Highway Engineering Aggregate Test Regulations" (JTG E42-2005), the technical indicators measured are shown in Table 2.

Table 2. Technical indexes of mineral filler

Type of mineral filler	Density (g/cm^3)	Hydrophilic coefficient (%)	Methylene blue coefficient (%)	Specific surface area	Average particle size (um)
Limestone	2.750	0.82	0.53	0.411	14.592

2.3. Rejuvenators

This article used Sika rejuvenator produced by Arkoma in France with the type of HT. Sika rejuvenator is a by-product composition of light components in the petroleum industry, and its main technical indicators are shown in Table 3.

Table 3. Basic technical indexes of Sika rejuvenator

Name of test project	Unit	Test Results
Viscosity (60°C)	Pa·s	109
Density	g·cm^{-3}	0.932
Saturation fraction	%	35.4
Aromatic fraction	%	28.6
Mass loss after RTFOT ageing	%	–2.5

As can be seen from Table 3 that the viscosity of Sika rejuvenator is lower, and the mass loss after RTFOT aging test is also lower, indicated that the rejuvenator is very safe with high temperature resistance and aging resistance.

2.4. Rejuvenated asphalt

In order to study the aging and rejuvenation of the actual pavement, the milling material recovered from the highway in Dingxi City, Gansu Province was extracted in the laboratory, which was recorded as RAP. At the same time, Sika rejuvenator was added to the extracted RAP aged asphalt mastic. Considering the serious aging of recycled RAP from practical engineering, the rejuvenator with content of 6%, 9% and 12% was added to RAP, and three kinds of rejuvenated asphalt samples with different rejuvenator content were prepared, which were recorded as RAP+6%, RAP+9% and RAP+12%, respectively. Rejuvenated asphalt's technical indicators are shown in Table 4.

Table 4. Basic technical indexes of rejuvenated asphalt

Asphalt model	Penetration (25°) /0.1 mm	Softening point/ °	Ductility (15°)/mm	Dynamic viscosity (60°)/Pa·s
RAP+6%	51	53.1	125	1130
RAP+9%	85	47.8	229	320
RAP+12%	129	42.9	356	136

3. Rheological model of rejuvenated asphalt mastic

3.1. Modified Burgers model

The basic mechanical property of asphalt mastic is viscoelasticity, so the viscoelastic model can be used to describe the interaction between internal elements of asphalt mastic [31]. In this paper, the Burgers contact model was used in the numerical simulation test of asphalt mastic, as shown in Eq. (3.1):

$$E_1E_2\sigma + (\eta_1E_1 + \eta_1E_2 + \eta_2E_1)\sigma + \eta_1\eta_2\sigma = E_1E_2\eta_1 + E_1\eta_1\eta_2\varepsilon \tag{3.1}$$

For asphalt materials, dynamic shear modulus and phase angle are the most commonly used viscoelastic parameters. A dynamic stress was applied to obtain the dynamic strain response, and the stress and strain were put into Eq. (3.1) to improve the constitutive equation of Burgers model, as shown in Eq. (3.2):

$$\frac{\varepsilon^*}{\sigma_0} = \frac{1}{K_m} + \frac{1}{i\omega C_m} + \frac{1}{K_k + i\omega C_k} \tag{3.2}$$

where: σ_0 – stress value at zero time, ω – angular frequency, and t – the time.

In this paper, the modified Burgers model of Eq. (3.2) was used to simulate the viscoelastic effect in rejuvenated asphalt mastic. The normal and tangential Burgers models correspond to the four parameters of the macroscopic Burgers model, and they were used in the contact between the particles of regenerated asphalt mastic. Therefore, the improved Burgers contact model was the microscopic expression of the Burgers model and reflected the material's mesoscopic viscoelasticity.

In Eq. (3.3) and Eq. (3.4), the parameters of the normal stiffness K_n and the tangential stiffness $K_s$of the discrete element were converted into a function of time, so as to characterize the DEM model dependency on time t.

$$K_n = \left[\frac{1}{K_{mn}} + \frac{\tau}{C_{mn}} + \frac{1}{K_{kn}}\left(1 - e^{\frac{-t}{\tau n}}\right)\right]^{-1} \tag{3.3}$$

$$K_s = \left[\frac{1}{K_{ms}} + \frac{\tau}{C_{ms}} + \frac{1}{K_{ks}}\left(1 - e^{\frac{-t}{\tau s}}\right)\right]^{-1} \tag{3.4}$$

3.2. Parameter fitting method of Burgers model

Based on the DSR test, the mesomechanic parameters of the Burgers model could be fitted. The relationship between dynamic modulus and Burgers model parameters is shown in Eq. (3.5):

$$|G^*| = \left[\left(\frac{1}{K_m} + \frac{K_k}{K_k^2 + \omega^2 \cdot C_k^2}\right)^2 + \left(\frac{1}{\omega C_m} + \frac{\omega \cdot C_k}{K_k^2 + \omega^2 \cdot C_k^2}\right)^2\right]^{-\frac{1}{2}} \tag{3.5}$$

where: G^* – predicted dynamic shear modulus, ω – angular frequency, $K_m(E_1)$, $C_m(\eta_1)$, $K_k(E_2)$, $C_k(\eta_2)$ – fitting parameters.

The relationship between the phase angle and the Burgers model parameters is shown in Eq. (3.6):

$$\delta = \tan^{-1}\left[\frac{1}{\omega \cdot C_m} + \frac{\omega C_k}{K_k^2 + \omega^2 \cdot C_k^2} \Big/ \frac{1}{K_m} + \frac{K_k}{K_k^2 + \omega^2 \cdot C_k^2}\right] \tag{3.6}$$

The following objective function can be established as shown in Eq. (3.7):

$$R = \sum_{j=1}^{n}\left(\left(\frac{G'(\omega_j)}{G'_0} - 1\right)^2 + \left(\frac{G''(\omega_j)}{G''_0} - 1\right)^2 + \left(\frac{\delta(\omega_j)}{\delta_0} - 1\right)^2\right) \tag{3.7}$$

where: G'_0, G''_0 – storage and loss modulus at different frequencies obtained by experiments, $G'_{(\omega)}, G''_{(\omega)}$ – storage and loss modulus at different frequencies calculated by the Burgers model parameters, n – number of frequency points measured in the experiment.

The four parameters $K_m(E_1)$, $C_m(\eta_1)$, $K_k(E_2)$, $C_k(\eta_2)$ of the model can be obtained by solving the minimum value of the objective function optimization. It's a process of repeated correction to obtain mesomechanical parameters by macro mechanical parameters of materials. Therefore, based on the macro mechanical parameters measured in the laboratory test, estimated and adjusted the mesomechanical parameters, and tested whether micro parameters are reasonable by comparing the results of virtual test and laboratory test, until the virtual test results can better conform to the actual data [3, 33].

4. Comparative analysis of macro DSR test and mesomechanical parameters of rejuvenated asphalt mastic

4.1. Analysis of DSR rheological test results of asphalt mastic

The DSR rheological test was carried out on the rejuvenated asphalt mastic, and the influences of various factors (rejuvenator content, temperature) on the rheological parameters were analyzed.

4.1.1. Effect of rejuvenator content on rheological properties of rejuvenated asphalt mastic

In order to explore the influence of different doses of rejuvenator on the changes in rheological parameters, taken KL-90 base asphalt as the reference asphalt, DSR test was carried out on rejuvenated asphalt samples (RAP+6%, RAP+9%, RAP+12%) with 6%, 9% and 12% rejuvenator added in recycled extracted asphalt RAP and RAP respectively at different temperatures. Each group of samples was tested three times to eliminate errors, and then the G^* curve was analyzed. The analysis result is shown in Figure 1.

As shown in Figure 1, the G^* of RAP was the largest at the same temperature, indicated that the modulus of asphalt mastic increased after long-term aging under natural conditions,

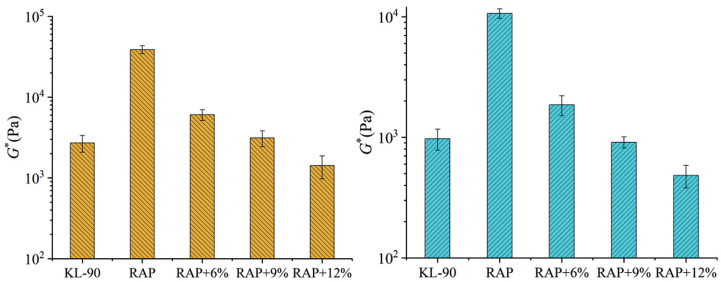

Fig. 1. Changes of complex shear modulus of aged asphalt mastic with different content of rejuvenator

and the deformation resistance was enhanced. The G^* of RAP decrease with the increase of the regenerant content. When the content of rejuvenator reached 9%, the G^* of rejuvenated asphalt mastic was basically close to that of KL-90 base asphalt. When the rejuvenator content reached 12%, the G^* value of RAP was lower than that of the original asphalt, Rejuvenator is a light component, and when it was added to aging asphalt mastic, it caused the rejuvenated asphalt mastic to soften and weakened the shear resistance. This phenomenon was more obvious with the increase of the rejuvenator content.

4.1.2. Effect of temperature on rheological properties of rejuvenated asphalt mastic

In order to analyze the high-temperature rheological properties of regenerated asphalt mastic, limestone mineral filler was added to RAP+ 9% to obtain rejuvenated asphalt mastic with different filler-asphalt ratio. KL-90 base asphalt mastic with the same mineral filler and filler-asphalt ratio was taken as the contrast sample. The temperature scanning test was carried out at the frequency of 10 rad/s and the temperature ranged from 40°C to 80°C. The influence of temperature on the high-temperature rheological properties of base asphalt mastic and rejuvenated asphalt mastic was analyzed. The complex shear modulus G^* under different temperatures is shown in Figure 2.

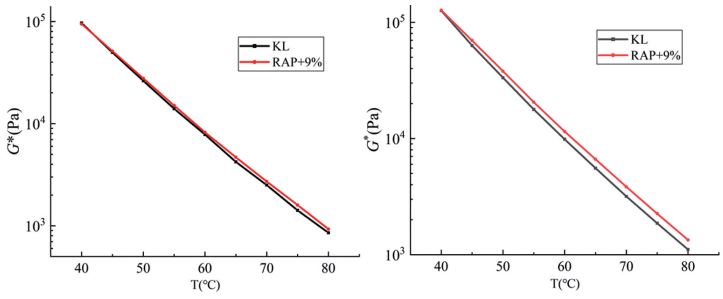

Fig. 2. Complex modulus of rejuvenated asphalt mastic under different temperatures

As shown in Figure 2, the complex shear modulus of rejuvenated asphalt mastic had the same trend as the original asphalt mastic with the change of temperature, and the G^* both decreased with the increase of temperature. However, the G^* of rejuvenated asphalt was larger than that of the base asphalt under the same temperature and filler-asphalt ratio, and the discrepancy became more significant as the temperature increased. The complex modulus of two kinds of asphalt mastic decreased with the increase of temperature, indicated that the higher the temperature, the stronger the fluidity of asphalt mastic and the worse the ability to resist deformation.

4.2. Analysis on influencing factors of mesomechanical parameters of rejuvenated asphalt mastic

Many factors affect the rheological properties of asphalt mastic, and the complex shear modulus of asphalt mastic is closely related to the four parameters of Burgers model. Therefore, it's significant to analyze the influence of various influencing factors on the four mesoscopic parameters. The relevant mathematical models were established to study the relationship between rheological parameters and mesomechanical parameters.

4.2.1. Effect of rejuvenator content on meso parameters of asphalt mastic

The rheological parameters of aged asphalt mastic were various with different amounts of rejuvenator. Different amounts of rejuvenator had different effects on the microscopic parameters E_1, η_1, E_2, and η_2 in Burgers model, the results are shown in Figure 3.

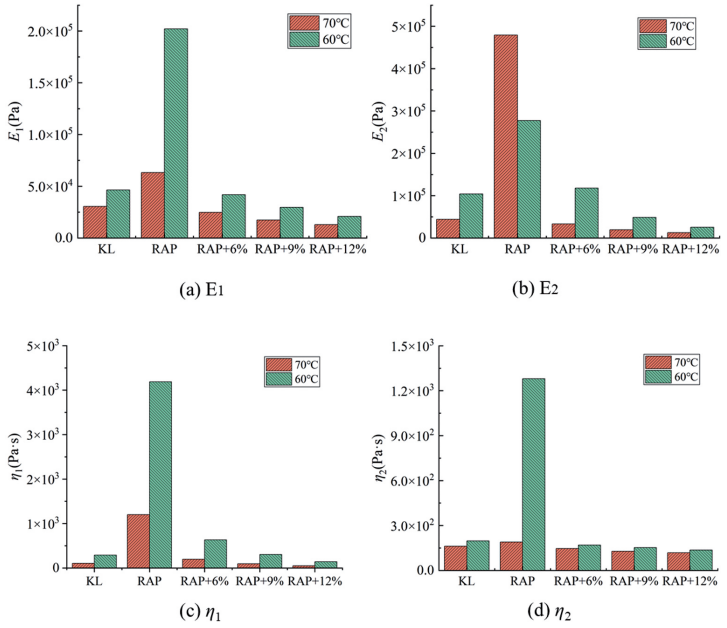

Fig. 3. Effect of rejuvenator agent content on meso parameters of rejuvenated asphalt mastic

As shown in Figure 3, at the same temperature, the meso parameters of RAP mastic were significantly higher than those of base asphalt and rejuvenated asphalt mastic. With the increase of rejuvenator content, the microscopic parameters of RAP mastic decreased.

4.2.2. Effect of temperature on meso parameters of asphalt mastic

In order to explore the influence of temperature on the mesomechanical model of asphalt mastic, the variation curves of the four parameters of base asphalt mastic and rejuvenated asphalt mastic with temperature were selected. It's filler-asphalt ratio was 0.9. The results are shown in Figure 4.

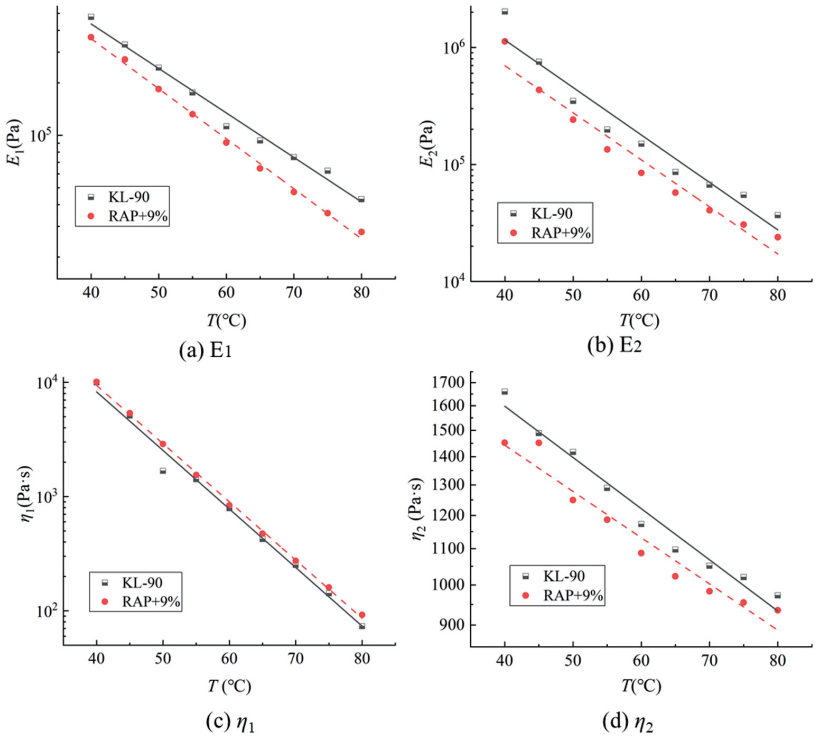

Fig. 4. Effect of temperature on meso parameters of rejuvenated asphalt mastic

As shown in Figure 4, the four parameter values of E_1, η_1, E_2, η_2 were linearly and negatively correlated with temperature. With the increase of temperature, the variations of the microscopic parameters of base asphalt mastic and rejuvenated mastic were consistent, which could be inferred that there was a mutual verification relationship between the microscopic parameters of asphalt mastic and the macroscopic complex shear modulus. Compared with the rejuvenated asphalt mastic, the E_1, η_1, and E_2 of the original asphalt mastic were greater than those of the rejuvenated asphalt mastic at the same temperature, while η_2 was just the opposite.

5. Validation of modified Burgers model parameters of rejuvenated asphalt mastic

From the above analysis, it could be seen that the mesoscopic parameters were closely related to the rheological parameters. The base asphalt mastic and rejuvenated asphalt mastic had the same variation law. The linear regression coefficients a_0, b_1, b_2, b_3, and b_4 were solved respectively. By inputting E_1, η_1, E_2, and η_2 on the MATLAB platform and calling the regression function based on the least square method, and then the linear fitting variance was obtained. Combined with the rheological property test data of asphalt mastic, the multiple linear relationships between complex shear modulus G^* and microscopic parameters E_1, E_2, η_1, and η_2 was established, as shown in Eq. (5.1):

$$y = 80.59 + 0.06E_1 + 4.43 \times 10^{-6}E_2 + \tau(7.74\eta_2 - 0.75\eta_1) \tag{5.1}$$

The least square method was used to solve the model, and the actual value of the statistical modulus sample points and the fitting value were mutually verified. The 95% confidence interval of the residual calculated by the regression function is shown in Figure 5.

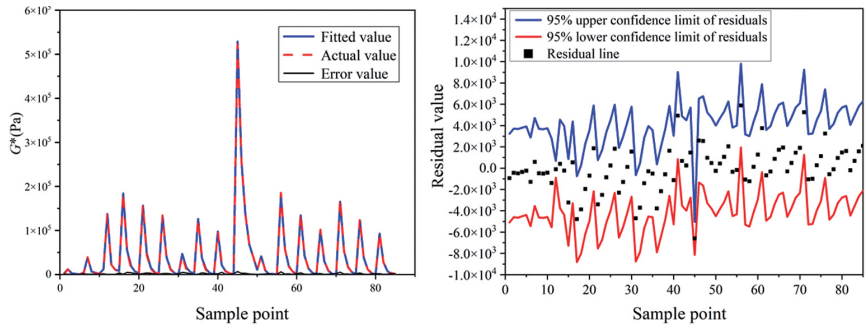

Fig. 5. Model fitting results

The calculated determination coefficients R^2 of G^* was 0.999, which was close to 1, indicated that the fitting variance was good, the fitting structure had sufficient credibility, and the linear relationship was established.

6. Discrete element simulation of rejuvenated asphalt mastic

6.1. Construction of DSR simulation test model

Asphalt mastic is a multiphase dispersion system. Therefore, in this study, graded spherical elements were used to simulate asphalt, irregular clumb was used to simulate mineral powder, and small balls with a certain particle size were bonded together to

simulate asphalt mastic, so that the mesomechanical characteristics of asphalt mastic were truly reflected.

6.1.1. Realization of Mineral Powder Particle Gradation

In this study, the winner 2000 laser diffraction particle size analyzer was used to conduct laser particle size tests on the selected mineral powder, and the particle size distribution of the test mineral powder was shown in Figure 6a. Figure 6a shows that the particle size of mineral filler presents a normal distribution. The particle size distribution curve of the mineral filler was converted into a particle size cumulative curve, which is the "experimental" curve in Figure 6b.

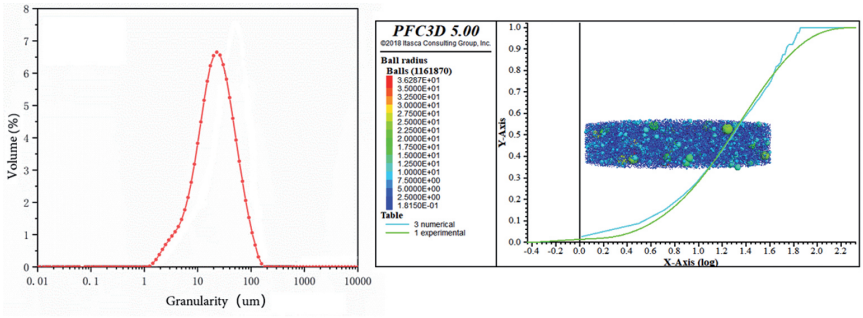

(a) (b)

Fig. 6. Particle size distribution curve of mineral filler

According to the cumulative particle size curve, the particle system was divided into multiple groups, and then the program was written in the fish language to randomly drop the particles, as shown in Figure 6b.

As can be seen in Figure 6b, the cumulative particle size curve of mineral filler in the laboratory test was basically consistent with that of the virtual particles.

6.1.2. Establishment of Asphalt Mastic Model

At present, the most commonly used methods for PFC 3D modeling are the moving boundary wall method, the expansion method, and the gravity drop method [34, 35]. The moving boundary wall method can well realize the dispersion of particles, and will not cause large overlaps of particles in local areas. Therefore, with the help of PFC3D software, this study used the moving boundary wall method to model the asphalt mastic, which used spherical particles to represent the asphalt, and the irregular rigid cluster (clump) template to represent the mineral filler. Through Eq. (6.1), the filler-asphalt ratio was converted to the volume ratio of the mineral filler particles to the asphalt particles. Then, the particles were randomly put through the command flow, and the mineral filler gradation was put according to the distribution. Finally, the overlapping particles were expanded to form a uniformly distributed asphalt mastic specimen, as shown in Figure 7.

$$\frac{V_{\text{Mineral powder}}}{V_{\text{Asphalt}}} = \frac{m_{\text{Mineral powder}}}{m_{\text{Asphalt}}} \times \frac{\rho_{\text{Asphalt}}}{\rho_{\text{Mineral powder}}} \tag{6.1}$$

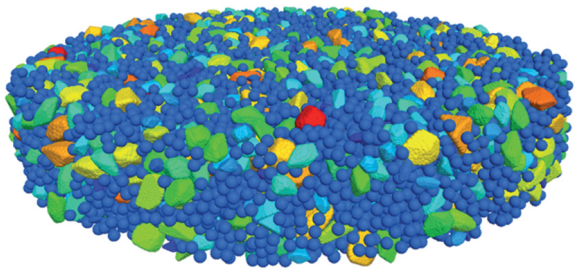

Fig. 7. Simulation diagram of DSR virtual specimen of asphalt mastic

According to the requirements, the sample of DSR test should adopt a cylinder of 25 mm in diameter and 1mm in height. Considering the number of particles in the numerical simulation, it was discretized into a cylindrical sample with a diameter of 5 mm and a height of 1 mm. Figure 8 and Figure 9 are the top view and front view of the DSR virtual sample. The asphalt mastic specimen was simulated from the microscopic particle scale, which could better represent the distribution of mineral filler in asphalt and the contact between them, and more intuitively represent the distribution of mineral filler in asphalt.

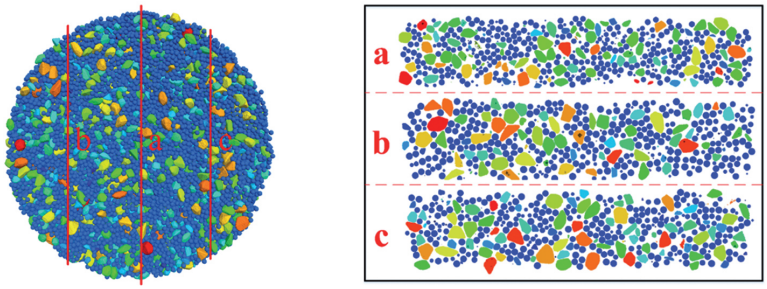

(a) Vertical view (b) Vertical view section

Fig. 8. Top view and section of DSR mastic sample

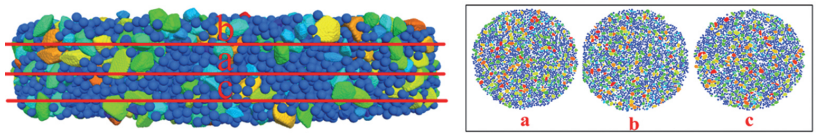

(a) Front view (b) Front view section

Fig. 9. Front view and section of DSR mastic sample

It can be seen in Figure 8 and Figure 9 that the shape of the mineral filler particles was diversified, which could better simulate the real mineral filler particles. The distribution of mineral filler particles and asphalt particles was evenly dispersed, and the mineral filler was coated by asphalt, thus formed a mineral filler-asphalt system.

6.2. Realization of DSR simulation test of rejuvenated asphalt mastic

The virtual test of asphalt mastic could be roughly divided into three steps. First, the virtual frequency scanning (FS) test of base asphalt was carried out to calibrate the meso contact parameters of DEM model. In Figure 10, the boundary and loading conditions were defined to simulate the real test conditions. The boundary conditions were applied to the specimen by the cylindrical wall, the rectangular wall was used as the loading plate, the lower loading plate was fixed, and the upper loading plate was oscillating to apply the load. Second, after the specimen was generated, the internal particles were contacted with each other according to the Burgers model, and the microscopic parameters could be obtained by fitting the Burgers model to the laboratory test results of the dynamic shear modulus. The fitting process was solved based on the minimization of the objective function, which could be used to predict the storage modulus, loss modulus and phase angle in the test frequency range. In the third step, the geometric parameters of the model were put into the DEM model, to perform a virtual FS test on the asphalt mastic, along with performing calibration, inputting parameters, and setting boundary conditions. Finally, the simulation results were compared with the test results to verify the simulation model.

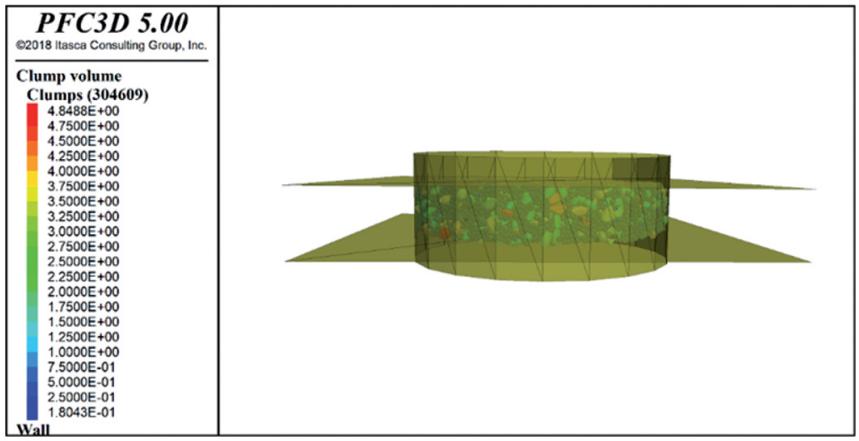

Fig. 10. DSR simulation test

The internal particle contact in asphalt mastic can be divided into three types: asphalt and asphalt contact, mineral filler and mineral filler contact, and asphalt and mineral filler contact. In the preliminary simulation, the contact parameters between asphalt and asphalt

were calibrated. The contact between mineral filler and mineral filler was defined according to the elastic contact in Eq. (6.2).

$$K_n = \frac{AE_r}{2R}; \quad K_s = \frac{K_n}{2(1+\upsilon)} \tag{6.2}$$

where: K_n – normal stiffness of the contact between the mineral filler and the mineral filler, K_s – tangential stiffness of the contact between the mineral filler and the mineral filler, E_r – reference modulus, A – contact area, υ – Poisson's ratio of the mineral filler.

The contact between asphalt and mineral filler was defined as the parallel combination of viscoelastic contact and elastic contact, as shown in Eq. (6.3):

$$\begin{aligned} &\frac{1}{K'_{ms}} = \frac{1}{K_s} + \frac{1}{K_{ms}}; \quad C'_{ms} = C_{ms}; \quad K'_{ks} = K_{ks}; \quad C'_{ks} = C_{ks}; \\ &\frac{1}{K'_{mn}} = \frac{1}{K_n} + \frac{1}{K_{mn}}; \quad C'_{mn} = C_{mn}; \quad K'_{kn} = K_{kn}; \quad C'_{kn} = C_{kn} \end{aligned} \tag{6.3}$$

where: K'_{ms}, K'_{ks}, K'_{mn}, and K'_{kn} – microscopic parameters of the contact between asphalt and mineral filler in Maxwell model, C'_{ms}, C'_{ks}, C'_{mn}, and C'_{kn} – meso parameters of the contact between asphalt and mineral filler in Kelvin model.

Finally, the geometric model and mesoscopic parameters of each component were added to the DEM simulation, and the virtual FS test was carried out to obtain the dynamic shear modulus of asphalt mastic. For verification, the simulation results were compared with the test results. Based on these two calibration models, the dynamic shear modulus of asphalt mastic with different filler concentrations was obtained from DEM simulation.

6.3. Analysis of DSR simulation results of rejuvenated asphalt mastic

Taking the above rejuvenated asphalt mastic as the simulation object, the virtual numerical simulation of frequency scanning at several specific frequencies was carried out at 64°, and the comparison between the virtual test results and the measured test results was obtained, as shown in Figure 11.

Figure 11 shows that the change trend of complex shear modulus and phase angle following angular velocity of asphalt mastic under different filler-asphalt ratio was consistent, and the logarithm of complex shear modulus and phase angle was also linearly correlated with the logarithm of angular frequency, and the linear correlation R^2 was above 0.98, which was consistent with the measured results. The results showed that the DSR test of rejuvenated asphalt mastic could be simulated by PFC, and the test results could be approximately predicted by adjusting the meso parameters. Therefore, it was inferred that different mesoscopic parameters could be obtained by adjusting the number, type and wall boundary of particles through PFC discrete element, so as the rheological parameters of rejuvenated asphalt mastic under different types, different filler-asphalt ratios and different external environments. These results could save a lot of time and laboratory testing workloads for later research.

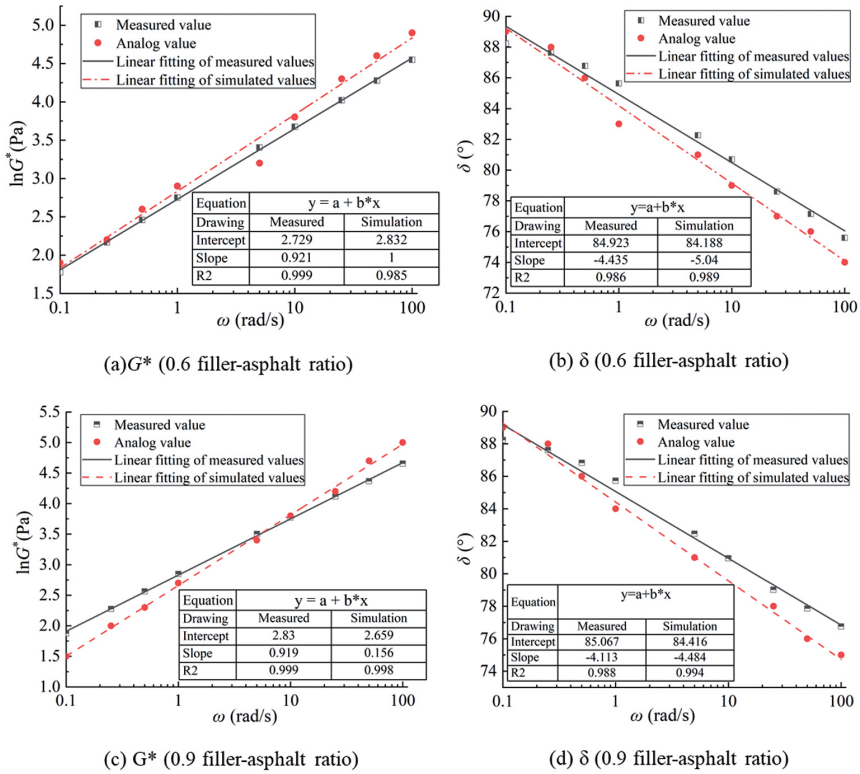

(a)G^* (0.6 filler-asphalt ratio)

(b) δ (0.6 filler-asphalt ratio)

(c) G* (0.9 filler-asphalt ratio)

(d) δ (0.9 filler-asphalt ratio)

Fig. 11. Virtual test results of rejuvenated asphalt mastic (R9+S mineral filler)

7. Conclusions

Through the comparative analysis of macro DSR test and micro mechanical parameters of rejuvenated asphalt mastic, it can be seen that the factors (the content of rejuvenator, temperature, etc.) that affect the rheological parameters of rejuvenated asphalt mastic also have the same influence on the mesomechanical parameters of rejuvenated asphalt mastic. With the increase of rejuvenator content, the meso parameters of RAP mastic decreased, and the mesomechanical parameters were linearly correlated with the filler-asphalt ratio. At the same time, the meso parameters of RAP mastic were significantly higher than those of base asphalt and rejuvenated asphalt mastic.

In order to explore the correlation between macro mechanics and micromechanical of regenerated asphalt mastic, the mathematical constitutive model of rheological parameter modulus and micromechanical parameters was established and verified in this paper. The model could be extended to predict the dynamic modulus of asphalt mastic in a wide frequency range and different powder-binder ratios.

The simulation results of DSR test of rejuvenated asphalt mastic by PFC were close to the actual test results, indicating that the prediction effect of the model was good. From

that, the complex shear modulus of rejuvenated asphalt mastic under different filler-asphalt ratios and external forces can be obtained by adjusting the particle flow, wall boundary and other conditions with PFC discrete element. It has important guiding significance for optimizing the laboratory test design and can save a lot of time and testing workload.

Acknowledgements

This study is sponsored by the National Natural Science Foundation of China (No. 51868047,52268070), Supported by Science and Technology Program of Gansu Province, (22JR5RA252), Gansu Provincial Higher Education Innovation Fund (2021A-021), Central University Key Research Platform Open Fund (300102211507) and Key scientific and technological projects in Gansu Province (2019-0201-GXC-0023).

References

[1] S.T. Lv, J. Liu, X.H. Peng, H.F. Liu, L. Hu, J. Yuan, and J.P. Wang, "Rheological and microscopic characteristics of bio-oil recycled asphalt", *Journal of Cleaner Production*, vol. 295, no. 1, art. no. 126449, 2021, doi: 10.1016/j.jclepro.2021.126449.

[2] J.Z. Liu, Q. Liu, S.Y. Wang, X.Y. Zhang, C.Y. Xiao, and B. Yu, "Molecular dynamics evaluation of activation mechanism of rejuvenator in reclaimed asphalt pavement (RAP) binder", *Construction and Building Materials*, vol. 298, no. 6, art. no. 123898, 2021, doi: 10.1016/j.conbuildmat.2021.123898.

[3] W.F. Ren, "Study on rheological properties of recycled asphalt with biological regeneration agent", *Journal of Highway and Transportation Research and Development*, vol. 16, no. 3, pp. 70–75, 2020.

[4] C.W. Wei, H.L. Zhang, and H.H. Duan, "The behaviour of rejuvenated SBS-modified asphalt incorporating catalytic-reactive compounded rejuvenator", *Road Materials and Pavement Design*, vol. 23, no. 2, pp. 433–444, 2022, doi: 10.1080/14680629.2020.1826344.

[5] D.M. Zhang, H.L. Zhang, and C.Z. Zhu, "Effect of different rejuvenators on the properties of aged SBS modified asphalt", *Petroleum Science and Technology*, vol. 35, no. 1, pp. 72–78, 2017, doi: 10.1080/10916466.2016.1248772.

[6] W. Sorociak, B. Grzesik, J. Bzówka, and P. Mieczkowski, "Asphalt concrete produced from rejuvenated reclaimed asphalt pavement (RAP)", *Archives of Civil Engineering*, vol. 66, no. 2, pp. 321–337, 2020, doi: 10.24425/ace.2020.131812.

[7] X.C. Yang, H.Z. Tang, X. Cai, K.H. Wu, W.K. Huang, Q. R. Zhang, and H. Li, "Evaluating reclaimed asphalt mixture homogeneity using force chain transferring stress efficiency", *Construction and Building Materials*, vol. 365, no. 1, art. no. 130050, 2023, doi: 10.1016/j.conbuildmat.2022.130050.

[8] D.A. Anderson, D.W. Christensen, H.U. Bahia, R.N. Sharma, M.G. Antel, and J.W. Button, *Binder characterization and evaluation, vol. 3. Physical characterization*. National Research Council, 1994.

[9] J.C. Petersen, R.E. Robertson, J.F. Branthaver, P.M. Harnsberger, J.J. Duvall, S.S. Kim, D.A. Anderson, D. Christiansen, and H. Bahia, *Binder characterization and evaluation*, vol. 1. National Research Council, 1994.

[10] J.C. Petersen, R.E. Robertson, J.F. Branthaver, P.M. Harnsberger, J.J. Duvall, S.S. Kim, D.A. Anderson, D. Christiansen, and H. Bahia, *Binder characterization and evaluation*, vol. 4. Test methods. National Research Council, 1994.

[11] H.L. Zhang, Z.H. Chen, G.Q. Xu, and C.J. Shi, "Evaluation of aging behaviors of asphalt binders through different rheological indices", *Fuel*, vol. 221, no. 1, pp. 78–88, 2018, doi: 10.1016/j.fuel.2018.02.087.

[12] J.S. Chen and C.J. Tsai, "Relating tensile, bending, and shear test data of asphalt binders to pavement performance", *Journal of Materials Engineering and Performance*, vol. 7, no. 4, pp. 805–811, 1998, doi: 10.1361/ 105994998770347404.

[13] J.S. Chen and C.J. Tsai, "How good are linear viscoelastic properties of asphalt binder to predict rutting and fatigue cracking?", *Journal of Materials Engineering and Performance*, vol. 8, no. 1, pp. 443–449, 1999, doi: 10.1361/105994999770346747.

[14] J. Wang, W. Zeng, and Y.C. Qin, "Experimental research on high temperature rheology of recycled asphalt", *Journal of Hefei University of Technology (Natural Science)*, vol. 41, no. 1, pp. 88–94, 2018, doi: 10.3969/j.issn.1003-5060.2018.01.017.

[15] S.P. Wu, L. Pang, L.T. Mo, Y.C. Chen, and G.J. Zhu, "Influence of aging on the evolution of structure, morphology and rheology of base and SBS modified bitumen", *Construction and Building Materials*, vol. 23, no. 2, pp. 1005–1010, 2009, doi: 10.1016/j.conbuildmat.2008.05.004.

[16] Z.Y. Zhang, J.N. Shen, P.C. Shi, and H. Zhu, "Micro-mechanism of asphalt aging based on nanomechanics and functional groups", *Journal of Highway and Transportation Research and Development*, vol. 34, no. 5, pp. 19–27, 2017.

[17] A. Abbas, E. Masad, T. Papagiannakis, and A. Shenoy, "Modelling asphalt mastic stiffness using discrete element analysis and micromechanics-based models", *International Journal of Pavement Engineering*, vol. 6, no. 2, pp. 137–146, 2005, doi: 10.1080/10298430500159040.

[18] A. Alhdabi, H.A. Nageim, F. Ruddock, and L. Seton, "Development of sustainable cold rolled surface course asphalt mixtures using waste fly ash and silica fume", *Journal of Materials in Civil Engineering*, vol. 26, no. 3, pp. 536–543, 2014, https://ascelibrary.org/doi/abs/10.1061/%28ASCE%29MT.1943-5533.0000843.

[19] M. Miljkovic and M. Radenberg, "Fracture behavior of bitumen emulsion mortar mixtures", *Construction and Building Materials*, vol. 62, no. 3, pp. 126–134, 2014, doi: 10.1016/j.conbuildmat.2014.03.034.

[20] X. Wang, "Experimental research on micro mechanism and performance of high proportion rap plant mixed hot recycled asphalt mixture", M.A. thesis, South China University of Technology, Guangzhou,2014.

[21] W.G. Buttlar, D. Bozkurt, and G.G. Alkhateeb, "Understanding asphalt mastic behavior through mesomechanics", *Transportation Research Record Journal of the Transportation Research Board*, vol. 1681, no. 1, pp. 157–169, 1999, doi: 10.3141/1681-19.

[22] T.F. Nian, J.G. Ge, P. Li, R. Guo, J.G. Li, and M. Wang, "Improved three-dimensional discrete modeling method and anti-cracking properties of asphalt mixture", *Construction and Building Materials*, vol. 321, no. 3, art. no. 126405, 2022, doi: 10.1016/j.conbuildmat.2022.126405.

[23] M. Miljković and M. Radenberg, "Fracture behavior of bitumen emulsion mortar mixture", *Construction and Building Materials*, vol. 62, pp. 126–134, 2014, doi: 10.1016/j.conbuildmat.2014.03.034.

[24] P.S. Kandhal, C.Y. Lynn, and F. Parker, "Characterization tests for mineral fillers related to performance of asphalt paving mixtures", *Transportation Research Record*, vol. 1638, no. 1, pp. 101–110,1998, doi: 10.3141/1638-12.

[25] H. Zhang, X. Liu, and Z. Qiao, "Study on Influencing Factors of viscosity and rheological properties of asphalt mastic", *Materials Reports*, vol. 33, no. 14, pp. 2381–2385, 2019, doi: 10.11896/cldb.17090309.

[26] L. Fan, J.M. Wei, Y.Z. Zhang, and L. Yu, "Effect of mineral powder on properties and mechanism of asphalt mastic", *Journal of Building Materials*, vol. 17, no. 6, pp. 1096–1101, 2014, doi: 10.3969/j.issn.1007-9629.2014.06.028.

[27] A. Abbas, E. Masad, T. Papagiannakis, and T. Harman, "Micromechanical modeling of the viscoelastic behavior of asphalt mixtures using the discrete-element method", *International Journal of Geomechanics*, vol. 7, no. 2, pp. 131-139, 2007, doi: 10.1061/(ASCE)1532-3641(2007)7:2(131).

[28] Y. Liu, P.F. Su, M.M. Li, H. Yao, J.F. Liu, M. Xu, X.D. Zhou, and Z.P. You, "How to achieve efficiency and accuracy in discrete element simulation of asphalt mixture: a DRF-based equivalent model for asphalt sand mortar", *Advances in Civil Engineering*, vol. 2020, no. 3, pp. 562–587, 2020, doi: 10.1155/2020/8855409.

[29] H. Feng, "Research on experimental characteristics of asphalt mortar based on viscoelastic theory", M.A. thesis, Changsha University of Technology, Changsha, 2008.

[30] H.L. Ma, "Micromechanical analysis of the effect of inorganic fillers on the mechanical properties of asphalt mortar", PhD. thesis, Jilin University, Changchun, 2013.

[31] Y.N. Xu, L.Y. Shan, and S. Tian, "Fractional derivative viscoelastic response model for asphalt binders", *Journal of Materials in Civil Engineering*, vol. 31, no. 6, art. no. 04019089, 2019, doi: 10.1061/(ASCE)MT.1943-5533.0002716.

[32] M. Baumgartner and H. Winter, "Determination of discrete relaxation and retardation time spectra from dynamic mechanical data", *Rheologica Acta*, vol. 28, pp. 511–519, 1989, doi: 10.1007/BF01332922.

[33] S.H. Li and Y.N. Wang, "Study on parameter selection method of three-dimensional discrete element calculation", *Chinese Journal of Rock Mechanics and Engineering*, vol. 23, no. 21, pp. 3642–3651, 2004, doi: 10.3321/j.issn:1000-6915.2004.21.014.

[34] Y.Q. Ling, Y.L. Yang, and C. Zhao, "Research on design of low porosity asphalt mixture based on PFC3D", *Journal of Chongqing Jiaotong University (Natural Sciences)*, vol. 39, no. 6, pp. 73–80, 2020.

[35] G. Dondi, A. Simone, V. Vignali, and G. Manganelli, "Discrete element modelling of influences of grain shape and angularity on performance of granular mixes for asphalts", *Procedia – Social and Behavioral Sciences*, vol. 53, no. 3, pp. 399–409, 2012, doi: 10.1016/j.sbspro.2012.09.891.

Received: 2022-10-22, Revised: 2023-02-28